Operations Update for the Deformable Mirror Demonstration Mission (DeMi) CubeSat

Rachel Morgan, Sophia K. Vlahakis, Greg Allan, Paula do Vale Pereira, Jennifer Gubner, Christian Haughwout, Bobby Holden, Thomas Murphy, Yinzi Xin[*], Kerri L. Cahoy[†]
MIT Department of Aeronautics and Astronautics

Ewan S. Douglas
Steward Observatory, University of Arizona

John Merk[‡], Danilo Roascio
Aurora Flight Sciences

Mark Egan, Gabor Furesz
MIT Kavli Institute

August 31, 2021

ABSTRACT

The Deformable Mirror Demonstration Mission (DeMi) CubeSat payload is a miniature space telescope designed to demonstrate Microelectromechanical Systems (MEMS) Deformable Mirror (DM) technology in space for the first time. MEMS DMs can provide high-precision wavefront control with a small form factor, low power device with the potential to be a key technology option for future space telescopes requiring adaptive optics. Applications of MEMS DMs in space include high-contrast imaging and optical communications.

The DeMi payload contains a 140-actuator MEMS DM from Boston Micromachines Corporation whose performance can be measured with both an image plane wavefront sensor and a Shack Hartmann wavefront sensor (SHWFS). The key DeMi mission goals are to measure individual actuator wavefront displacement contributions to a precision of 12 nm and correct both static and dynamic wavefront errors in space to less than 100 nm RMS error. The DeMi mission has raised the Technology Readiness Level (TRL) of MEMS DM technology from a 5 to a 9.

This paper summarizes payload data from the first year of in-space operations after briefly summarizing the DeMi optical payload design, calibration, integration and environmental testing results. Ground testing data shows that the DeMi SHWFS can measure individual actuator deflections on the MEMS DM to within 10 nm of interferometric calibration measurements and ground and space data can meet the 12 nm precision requirement for actuator deflection voltages between 0-120 V [1]. Individual actuator measurements from space operations show the MEMS DM actuating in space with similar performance and measurement uncertainty to ground data. Differences between repeated measurements of individual actuators have a standard deviation of 3-16 nm. Data from inital wavefront control experiments show the DeMi payload correcting wavefront errors in space to less than 150 nm RMS.

1. INTRODUCTION

The Deformable Mirror Demonstration Mission (DeMi) CubeSat mission is demonstrating a Microelectromechanical Systems (MEMS) Deformable Mirror (DM) in space for the first time. The optical payload is a miniature space telescope with an adaptive optics instrument designed to demonstrate a 140-actuator MEMS DM from Boston Micromachines Corporation. This paper presents data on the DM performance over the first year of on-orbit operations from July 2020 to July 2021.

[*] Currently California Institute of Technology Department of Physics
[†] Also MIT Department of Earth Atmospheric and Planetary Sciences
[‡] Currently Draper Laboratory

DMs are used to correct wavefront errors in optical systems for applications such as astronomy [2], space situational awareness [3], re-configurable optics [4], laser communications, and life sciences [5]. DMs are a key part of an adaptive optics system, which measures the shape of optical wavefront errors and controls the DM shape to compensate for them and provide a higher quality image.

High contrast imaging of exoplanets is an exciting and challenging application for DMs. Capturing images of exoplanets enables precise astrometric and spectroscopic measurements for orbital and atmospheric characterization [6, 7, 8, 9]. Imaging an Earth-like exoplanet around a Sun-like star using a space telescope with a coronagraph instrument will require extremely precise wavefront control to meet the required contrast limit of 10^{-10} [2, 10, 11, 12, 13]. This will require adaptive optics systems capable of picometer-level wavefront control [10] because residual wavefront errors cause speckles in the science image that can obsure the exoplanet signal [6].

MEMS DMs are a promising technology option for wavefront control in space because of their small actuator pitch ($\sim 300-400$ μm), small form factor, large stroke, and low power draw [14, 15, 16]. The high actuator density of MEMS DMs allows high-spatial resolution wavefront control with a smaller optical system, which is important for Size, Weight, and Power (SWaP)-constrained systems such as space telescopes. MEMS DMs are made out of layers of polysilicon films that are etched to form actuators that are individually addressable through wire channels on a ceramic carrier [5]. The DM surface shape is electrostatically controlled by sending voltage commands to each actuator. MEMS DMs have been investigated and flown in the near space environment on sounding rockets [17], high-altitude ballons [18, 19], and undergone space-relevant testing on the ground as summarized in [16]. The goal of the DeMi CubeSat mission is to show that MEMS DMs can operate in space after experiencing launch dynamics and the low-Earth orbit (LEO) radiation and thermal environment.

1.1 DeMi Mission Overview

The DeMi payload was designed and built by the Massachusetts Institute of Technology (MIT) to fly in a 6U CubeSat bus from Blue Canyon Technologies. The spacecraft underwent environmental testing in Oct-Dec 2019, launched to the International Space Station in February of 2020, and was deployed into orbit on July 13 2020. The first on-orbit payload data confirming DM actuation in space was collected and downlinked in August of 2020 [1]. The key DeMi mission goals are to measure individual DM actuator wavefront displacement contributions to a precision of 12 nm, measure low order optical aberrations to $\lambda/10$ accuracy and $\lambda/50$ precision, and correct both static and dynamic wavefront errors to less than 100 nm RMS error [20]. The DeMi mission has raised the Technology Readiness Level (TRL) of MEMS DM technology from a 5 to a 9 for future space telescope applications. More details on the mission and payload design and development can be found in previous publications [1, 21, 22, 23, 24, 25, 26, 27, 28, 29, 30, 31].

The DeMi optical payload is a miniature space telescope with an adaptive optics instrument. The payload has both a Shack-Hartmann wavefront sensor (SHWFS) to measure wavefront shape and an image plane wavefront sensor to measure the system point-spread function (PSF). A diagram of the optical payload is shown in Figure 1. The DeMi payload design and alignment procedure is described in detail in previous publications [32, 27, 33].

Two Rasperry Pi 3 single-board compute modules are used as payload computers, with each computer interfacing with one of the wavefront sensor cameras. The original DM driver electronics were too large to fit in a CubeSat payload, so miniaturized DM driver electronics based on commercial components were developed for this mission [34].

The DeMi payload has internal and external observation modes. For internal observations, a calibration laser source illuminates the DM and is measured on the wavefront sensors in order to provide measurements of the DM surface. Internal operations are used to measure DM actuator deflections, applied DM shapes, and wavefront control experiments. For external observations, the spacecraft slews to point at a star and the starlight is collected by the primary mirror. During external operations, the DM can be used for tip-tilt pointing compensation and for wavefront control experiments.

This paper presents data from internal operations using the SHWFS. The SHWFS consists of a lenslet array and a CMOS detector. The lenslet array focuses incident collimated light into an array of spots on the detector. The displacement of these spots from their nominal position represents the slope of the corresponding portion of the incident wavefront. The payload records the spot centroid displacements, which are downlinked and used for zonal reconstruction of the wavefront shape with the Southwell geometry using the Moore-Penrose pseudoinverse approach [35, 36].

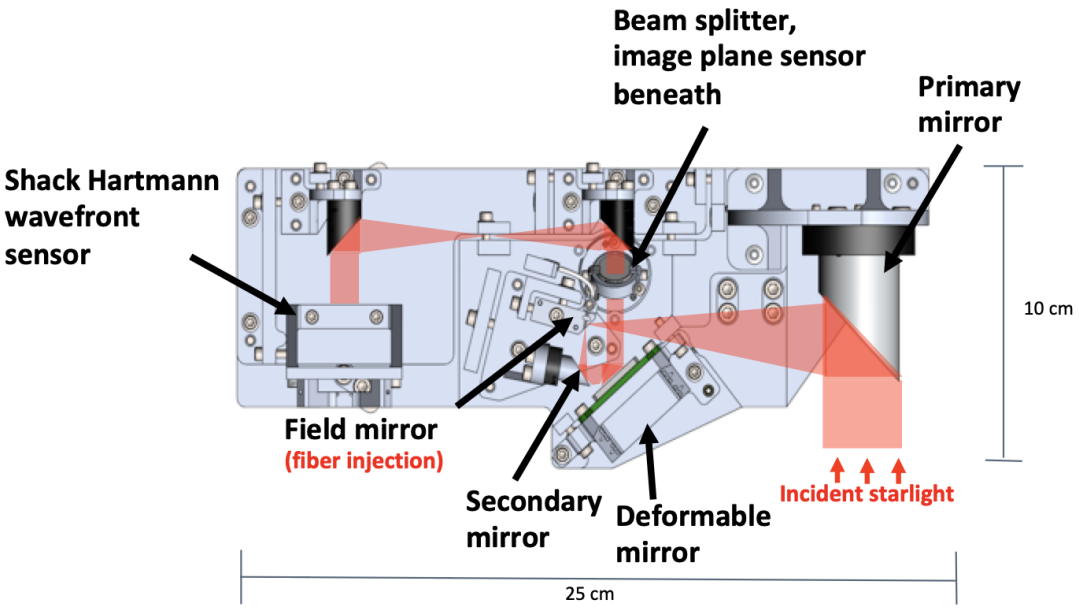

Fig. 1: DeMi optical payload diagram.

2. PAYLOAD DATA OVERVIEW

There are two types of SHWFS data presented in this paper, actuator deflection measurement data and wavefront control experiment data. Actuator deflection measurement data is collected by poking (commanding a single actuator to a specified voltage) each actuator on the DM and measuring the SHWFS centroid displacements. The array of centroid displacements for each poked actuator is downlinked and used to measure the deflection of each actuator. Zonal reconstruction converts the centroid displacement measurements to a wavefront reconstruction by solving the matrix problem:

$$As = Dw. \tag{1}$$

Where A is a matrix representing the averaging of slope measurements sampled by the lenslet array, s is the vector of measured centroid displacements, D is a matrix representing the derivative of the wavefront vector, and w is the wavefront vector. This equation is solved for the wavefront vector w by calculating the pseudoinverse (denoted by †) of the matrix D:

$$w = D^{\dagger}As^{T}. \tag{2}$$

The wavefront reconstruction is divided by two to give the DM surface measurement to account for the reflection off the DM. A 2-dimensional Gaussian function is fit to the DM surface measurement and the amplitude of the Gaussian fit gives the actuator deflection measurement. The standard deviation of the residual (wavefront reconstruction minus Gaussian fit) gives the deflection measurement uncertainty.

The second data type is wavefront control (WFC) experiment data, where the SHWFS is used for closed-loop control of the DM. First, a calibration matrix is calculated by poking each actuator by 30V from a default flat map and recording a matrix of spot displacements by poked actuator number. The calibration matrix is inverted to form the control transfer matrix. This transfer matrix is used for closed loop mirror control to steer the spot displacements to zero, correcting misalignments in the optical system due to thermal and mechanical variations since launch. A single iteration of closed loop mirror control starts with the payload capturing an image on the SHWFS camera and calculating centroids for the spots. These spot displacements are converted to DM voltage controls using the formula:

$$C = -gTs \tag{3}$$

where C is a vector of control commands, g is the control gain, T is the transfer matrix, and s is the vector of SHWFS centroid displacements. The calculated DM commands are applied to the DM, and then another iteration begins. There is a pause of 100 ms between WFC iterations to prevent the payload computer (Raspberry Pi 3 Compute Module) from overheating while processing the data. The spot displacements at each iteration are saved and downlinked for analysis. The WFC data is analyzed by reconstructing the wavefront at each iteration from the measured spot centroid displacements. A summary of the WFC experiment concept of operations used for the data presented in this paper is shown in Figure 2.

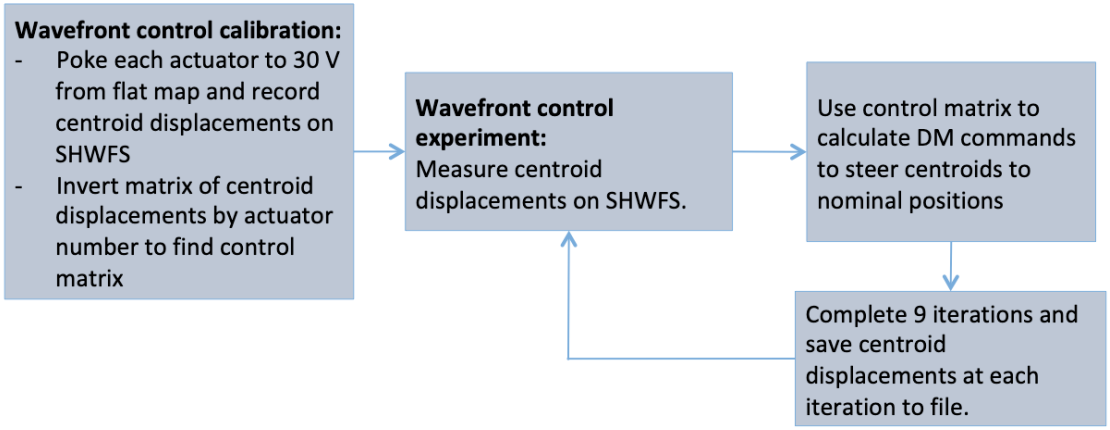

Fig. 2: Summary of WFC experiment concept of operations used for data presented in this paper. Future operations will involve WFC experiments with more iterations.

2.1 Payload Calibration

The DeMi payload alignment, spacecraft environmental testing, and data calibration are summarized in [1]. The data collected during ground testing is used to calibrate the SHWFS actuator deflection measurement data. First, interferometer measurements of single actuator pokes were collected using the MIT miniaturized DM driver and the original DM driver from the mirror manufacturer. These measurements showed that the miniature DM driver developed for the DeMi mission operates with similar performance to the original manufacturer driver [1]. An optical diffraction model is used to predict a measurement calibration factor α of 0.9 to account for the angle of the DM in the payload design [32, 1]. This calibration factor scales the interferometer measurements which are taken with the DM at normal incidence so they can be compared with payload SHFWS measurements of the DM at an angle (actual actuator deflection is the measured actuator deflection divided by this calibration factor). Single actuator pokes measured with the SHWFS are compared to interferometer measurements of the DM and find good agreement [1]. Ground testing data analysis shows that the DeMi SHWFS can measure individual DM actuator deflections to within 10 nm of interferometer measurements and can meet the 12 nm precision mission requirement for actuation voltages of 0-120 V. A sample of relevant ground data to compare orbital results with is shown in Table 1.

3. SPACE OPERATIONS AND DATA

On-orbit operations began in July of 2020. The first month of operations was focused on establishing communications with both ground stations. The DeMi mission is operated by MIT using a combination of a low-rate radio link between a ground station on MIT campus and a Lithium radio on the spacecraft and a high-rate radio link between a ground station at NASA Wallops Flight Facility and a Cadet radio on the spacecraft. After regular communications was established and spacecraft commissioning completed, payload operations began. This section summarizes early payload operations and lessons learned and presents DeMi payload data from space.

Table 1: Summary of single actuator poke measurements from ground testing with the DeMi Shack-Hartmann wavefront sensor (SHWFS) and interferometer calibration measurements.

Commanded poke voltage	**SHWFS mean poke measurement (uncertainty) [nm]**	**Mean interferometer calibration measurement (uncertainty) including α calibration factor [nm]**
30V	35 (5)	33 (5)
60V	147 (11)	153 (10)

3.1 Early Payload Operations

The goal of early payload operations was to confirm that the payload computers, cameras, laser, DM driver, and DM survived launch and deployment intact. To check this, actuator deflection data was collected and downlinked in August 2020 with the internal laser source turned on as presented in [1], which confirmed that the payload was operating properly. An image of the spotfield on the SHWFS was captured with the internal laser source turned on in order to check that the system alignment didn not change considerably from the ground measurements. The spotfield is shown in Figure 3 with the ground spot centroid locations marked with red circles. The image shows that the spots have moved a small amount since pre-launch testing due to changes in alignment, but not enough to interfere with SHWFS operation. The ground centroid locations are used to partition the camera image into regions to calculate spot centroids over and as a baseline for WFC experiements. DM actuator poke measurements measure baseline spot locations each time an experiment is run, so spot motion does not impact the ability to measure DM actuator deflections.

Early payload operations taught the team many valuable lessons. First, payload data captured when the spacecraft is in daylight had too much stray light from the ground to be used to characterize the DM. The DeMi operations team therefore schedules all payload operation commands to execute when the spacecraft is in eclipse. Second, the DeMi payload computers are Raspberry Pi 3 compute modules which tend to heat up when operated in vacuum. This heating leads to throttling of the computers when the payload is left on for a long time and the Pi board temperature rises above 80° C. Attempts to capture DM actuator data when the Pi temperature is this high show that the DM does not actuate under these conditions. The throttling of the Pi due to the high temperature is believed to interfere with the timing of commands sent to the DM driver, which rejects these commands and does not move the DM actuators. To compensate for this, the DeMi team now powers the payload off for an hour or more before scheduling payload commands to allow the payload computer to cool off and mitigate the impact of Pi throttling on DM operations.

Mechanical issues with the NASA WFF high-rate ground station from Fall 2020 - Spring 2021 limited the downlinking of payload data during the first year of operations. The DeMi team wrote new software for the ground station to be able to receive payload data over the Lithium low-rate radio link to the MIT ground station. This link is slower and lossier than the Cadet-WFF high-rate link but provides the team access to payload data when the high-rate link is out of commission. Current payload operations is focused on providing measurements of DM actuator deflections at different command voltages at different times on-orbit to show that the DM is operating consistently and reliably in space. Preliminary results from these measurements are summarized in Section 3.2. The DeMi team has also captured experiments using the SHWFS and the DM for wavefront control, summarized in Section 3.3.

3.2 DM Actuator Deflection Data

DM actuator deflection data has been collected with the DeMi SHWFS in space for a variety of commanded voltages. The data is processed by reconstructing the wavefront from the centroid displacements recorded when each actuator is deflected. Bit errors on downlink caused rare unphysical centroid values in some files, which were filtered from the files before processing the data. An example plot of the centroid displacements measured and the corresponding wavefront reconstruction for Actuator 86 commanded to 150 V is shown in Figure 4 (note that the centroid displacements are exaggerated in the plot for visibility). A 2D Gaussian function is fit to the wavefront reconstruction in order to extract the actuator deflection amount. The amplitude of the 2D Gaussian function gives the actuator deflection measurement in units of wavefront error, which is divided by two to give the actual actuator deflection measurement. The standard deviation of the residual (wavefront reconstruction - Gaussian fit) gives the measurement uncertainty for each actuator deflection measurement. An example Gaussian fit and residual uncertainty measurement for Actuator 86 poked to 150 V is shown in Figure 5.

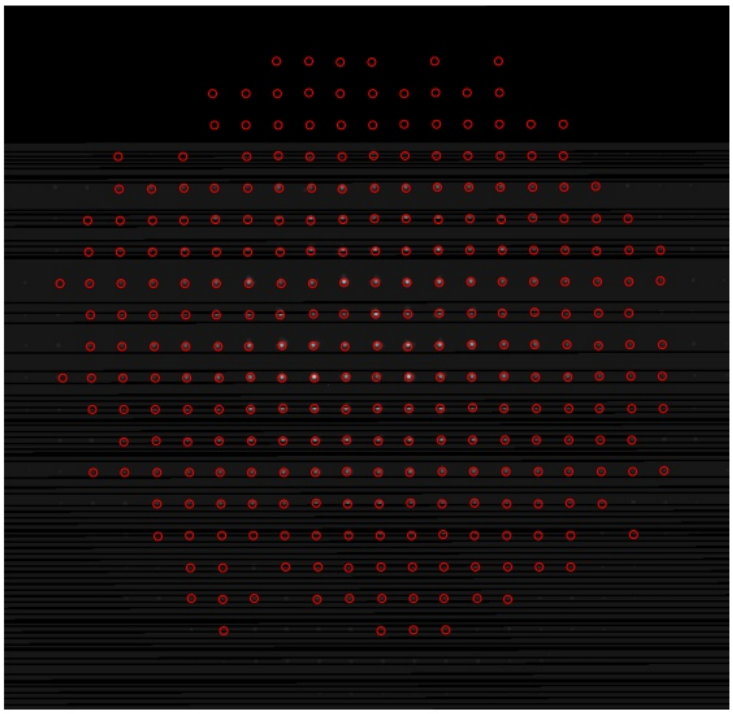

Fig. 3: SHWFS spotfield captured in space with the internal laser source on March 16, 2021. Gray/white spots are SHWFS lenslet spots and red circles denote the locations of spot centroids from ground testing. Black stripes are due to missing data from dropped packets during file staging/downlink. These results indicate that the alignment has shifted slightly since pre-launch testing but the spots have not moved enough to interfere with SHWFS operation.

Actuator deflection measurements from several on-orbit experiments at a variety of commanded poke voltages are shown in Figure 6 in addition to actuator deflection data collected during ground environmental testing (see [1] for more information on environmental testing data). Actuator measurements displayed are filtered to only include actuators without missing data from incomplete downlinks. The data is labeled according to the stage of environmental testing and recorded payload temperature when the data was collected. Data from on-orbit operations is labeled as"Space data" with a range of expected payload temperatures. The actual payload temperatures are not known for most actuator measurement experiments because they were scheduled to execute at times when the spacecraft would be in eclipse and not able to downlink spacecraft telemetry to a ground station. The expected payload temperature range is determined by analyzing telemetry from satellite communications passes when the spacecraft is in eclipse and payload temperature data is available. From this analysis, the payload temperature in eclipse is typically about 15° C but can vary between 10-18° C. As of July 2021, space data indicates that none of the actuators visible to the SHWFS with the internal laser source have stopped responding to voltage commands since launch.

Actuator deflection measurements from on-orbit operations agree very well with ground environmental testing measurements and calibration measurements from the mirror manufacturer. The actuator deflection measurements appear to have a dependence on payload temperature, with lower temperatures leading to dampened actuator deflection measurements. Ground testing data is available with payload temperatures of 6° and 24 - 29° C, and space data is expected to have payload temperatures of 10 - 18° C, which is higher than the cold dwell data from thermal vacuum testing

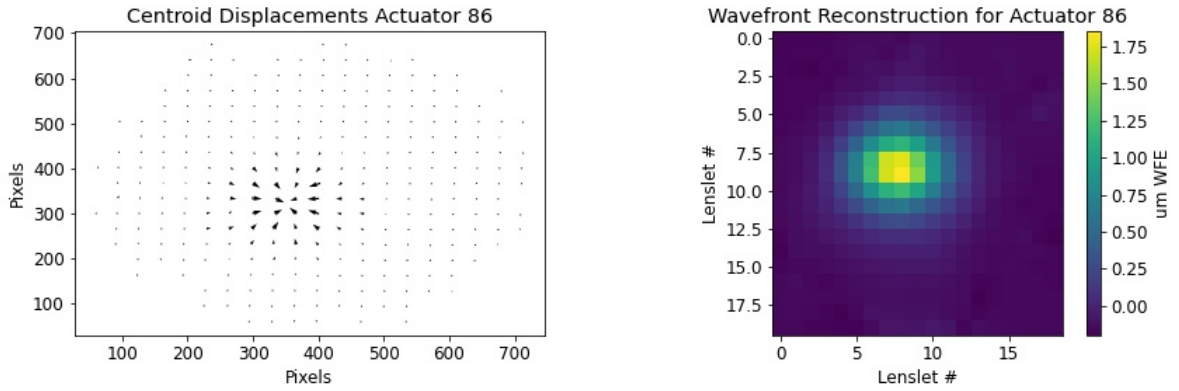

Fig. 4: Centroid displacement plot (left) and wavefront reconstruction (right) for actuator 86 poked to 150 V from 0 V baseline. This actuator deflection measurement data was collected on-orbit on June 24, 2021. The spots in the centroid displacement plot denote the baseline spot locations and the arrows point in the direction of spot centroid motion when the actuator is deflected. The magnitudes of the arrows on the centroid displacement plot are exaggerated so the spot displacements are clearer by eye. The wavefront reconstruction is displayed in units of wavefront error, which is divided by two to give the surface measurement of the DM.

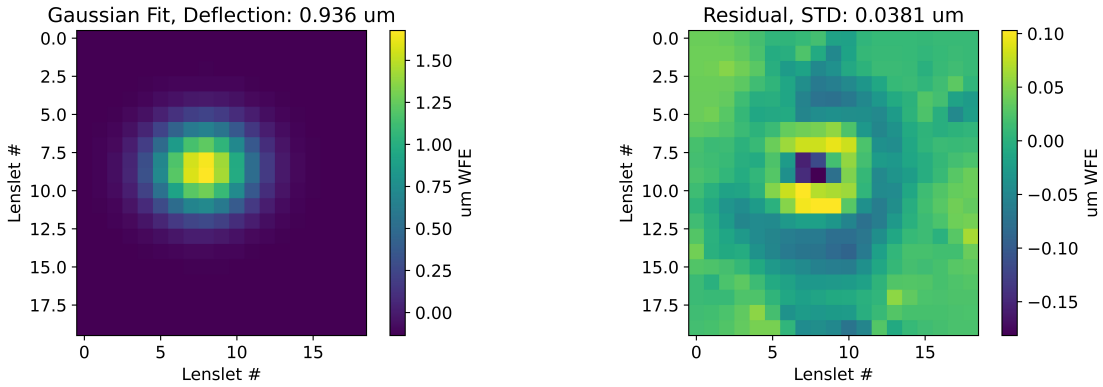

Fig. 5: Gaussian fit (left) and residual (right) for a SHWFS measurement of Actuator 86 commanded to 150 V. The corresponding wavefront reconstruction for this measurement is shown in Figure 4. The measured actuator deflection was 0.936 um and the measurement uncertainty (given by the standard deviation of the residual) was 19 nm. Note these plots are shown in units of wavefront error, values are divided by two to give the surface measurement of the DM.

(TVAC) at 6° C but colder than all of the other ground data experiments. The space payload data shows actuator deflection measurements that are higher than the coldest ground experiment [TVAC at 6° C] but lower than the other measurements [all other ground data, 24 - 29° C], which aligns with the observed trend that lower temperatures lead to lower DM actuator deflection measurements. The difference in measurements from high/low temperatures is observed to be around 200 nm for commanded poke voltages of 150 V. The DeMi team has modeled the expected thermal effects on the SHWFS and concluded that thermal expansion/contraction in the optical system cannot explain the magnitude of the observed difference in actuator deflection measurements. The observed trend could be due to thermal effects in the MEMS DM materials or potentially the DM driver electronics, though the DM driver components are not expected to have a strong thermal dependence according to manufacturer data. More testing is planned using a MEMS DM and MIT driver on the ground in a thermal chamber in order to understand the cause of this observed behavior.

Figure 7 shows the median actuator measurement uncertainties from each actuator poke experiment shown in Figure 6. Results show that the measurement uncertainty increases with increasing commanded poke voltage. The DeMi SHWFS can meet the 12 nm actuator deflection measurement precision requirement for commanded poke voltages

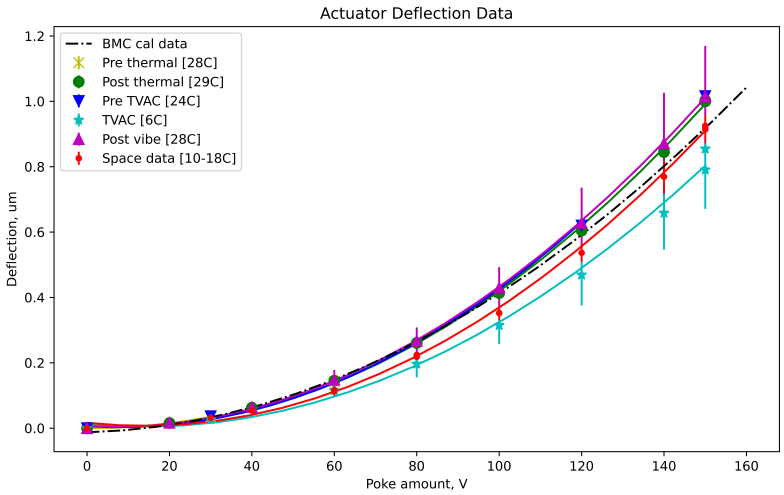

Fig. 6: Summary of actuator deflection data from space operations and ground environmental testing. Data markers indicate the median of all actuators measured during each experiment, error bars denote the standard deviation of the actuator measurements, and solid lines display quadratic fits to the measurement data. Data is colored/labeled according to the phase of environmental testing/operations it was collected during and the corresponding payload temperature as recorded by a thermistor installed on the optics bench. The black dashed line shows interferometric measurements of the DM provided by Boston Micromachines Corporation (BMC) for calibration. The pre-thermal, post-thermal, pre-thermal vacuum (TVAC), and post vibe measurements are all very similar to each other and are the group of overlapping lines that lie slightly above the dashed black BMC calibration data line in the chart. The blue TVAC cold dwell line shows the lowest deflection measurements, and the red space data line lies between the TVAC cold dwell data and the rest of the environmental testing measurements. These results indicate that actuator deflection measurements with the DeMi SHWFS have a thermal dependence, with lower temperatures resulting in slightly lower actuator deflection measurements.

of up to 120 V for well-illuminated DM actuators. The measurement uncertainty is greater for higher commanded voltages or actuators that are less well-illuminated by the internal laser source, up to $\sim$ 30 nm for the largest commanded poke voltage. These results show that the DeMi SHWFS has the same level of measurement uncertainty in space compared to ground data.

Actuator deflection measurements with the same commanded voltage from different times on orbit are compared to assess the repeatability of the measurements. These repeat measurements are summarized in Table 2 which lists the commanded actuator poke voltage, the dates of the experiments being compared, and the mean and standard deviation of the absolute value of the difference between individual actuator deflection measurements. The repeated measurement data agrees very well, with the standard deviation of the differences between individual actuator measurements ranging from 3-16 nm for different experiment types.

3.3 Wavefront Control Experiments

Eight WFC experiments were run with the DeMi SHWFS using the internal laser source in June 2021. Each WFC experiment consists of 9 iterations of measuring centroid displacements and calculating/applying the appropriate DM commands to correct for the measured wavefront error using a control gain of 0.3. The goal of the WFC experiments is to be able to correct for any misalignments in the optical system that may have occured since pre-launch testing. Misalignments in space could be due to thermal drift on-orbit or mechanical vibrations during launch, and are measured by comparing the payload SHWFS centroid displacements to their nominal pre-launch positions. At each iteration, the centroid displacements from the nominal pre-launch positions are recorded to a file which is downlinked and used to reconstruct the wavefronts from the experiment. Example reconstructions of the first and last iteration from a WFC experiment on June 17, 2021 are shown in Figure 8. To our knowledge, this is the first experimental data demonstrating wavefront control on-orbit with a MEMS DM.

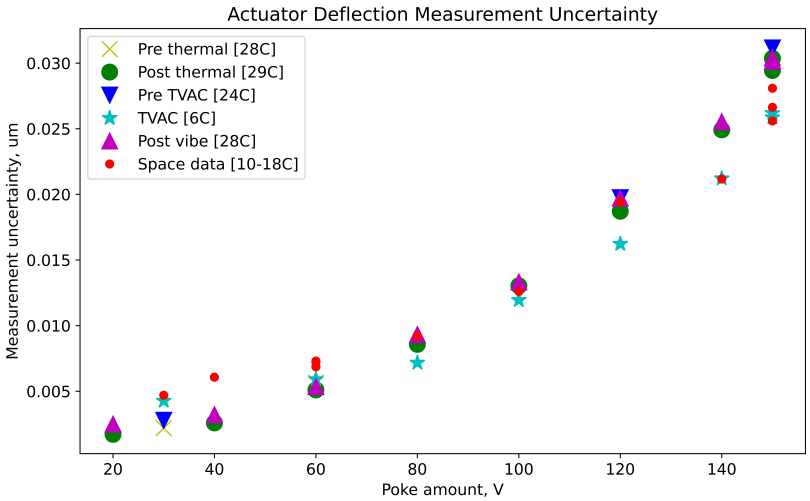

Fig. 7: Measurement uncertainties for actuator deflection measurements shown in Figure 6. Uncertainty is given by the standard deviation of the residual of the 2D Gaussian fit to the wavefront reconstruction of actuator deflection measurements in DM surface units (not wavefront error). Values displayed are the median of all measured actuator uncertainties during each experiment. Results indicate that the measurement uncertainty increases with commanded pok e voltage and that the DeMi SHWFS measurements have similar uncertainties in space compared to ground data.

Table 2: Summary of repeated actuator deflection measurements with the DeMi SHWFS. The commanded voltage and DM reference to measure spot displacements from (either an on-board flat map or 0 V on all actuators) are used to identify the experiment type, and the dates of experiments describe the time period between repeated measurements. The mean and standard deviation of the differences between the two experiments (earlier - later measurement) are displayed.

Commanded voltage/reference	**Dates of experiments**	**Mean difference (standard deviation) [nm]**
60 V ref. flat	August 4 2020, June 12 2021	6 (16)
60 V ref. zero	June 3 2021, June 5 2021	2 (4)
80 V ref. zero	August 9 2021, August 16 2021	2 (3)
150 V ref. zero	Different times on June 24 2021	4 (7)

The root-mean-square (RMS) of the wavefront reconstruction is used to assess the level of wavefront error during each WFC experiment. A plot of the wavefront reconstruction RMS error at each WFC iteration for each WFC experiment is shown in Figure 9. In each of the experiments, the DeMi payload was able to reduce the RMS wavefront error from $\sim$ 450 nm to less than 150 nm. The DeMi mission goal is to reduce the RMS wavefront error to less than 100 nm. The DeMi team hopes to reach this requirement by running more WFC experiments with a higher number of iterations to reduce the wavefront error further.

4. CONCLUSION

The DeMi mission is ongoing, with more payload experiments planned in the upcoming months. The DeMi spacecraft launched to the International Space Station in February of 2020 and has been operating on-orbit since July of 2020. The DeMi MEMS DM has been demonstrated to work after over 1.5 years in space and over 1 year of orbital operations, surpassing the mission requirement for 1 year of orbital operations. Data from the DeMi technology demonstration mission will inform designs for future spacecraft instruments requiring wavefront control with MEMS DMs for applications such as high-contrast imaging and laser communications. The DeMi mission is an exciting

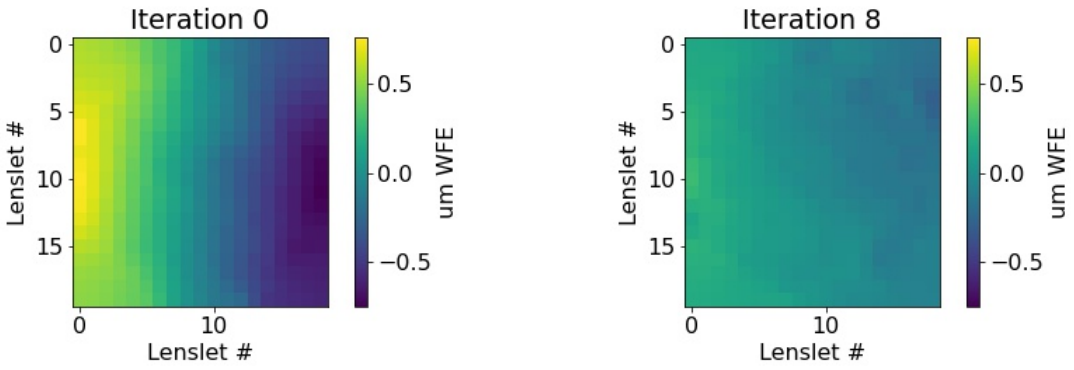

Fig. 8: Wavefront reconstructions from the first (left) and last (right) iterations of a wavefront control experiment run on June 17, 2021. The DeMi payload successfully reduced the RMS wavefront error in the optical system from $\sim$ 450 nm to $\sim$ 150 nm over 9 iterations of wavefront control.

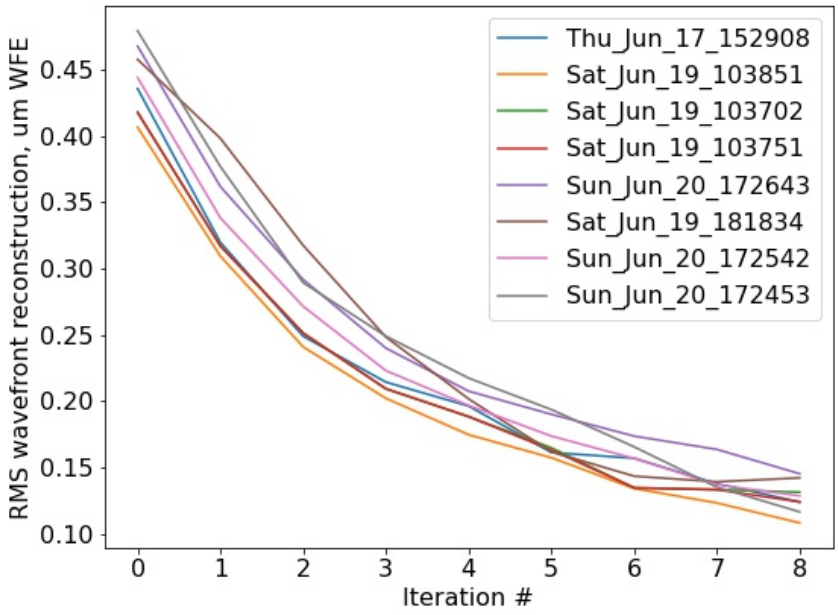

Fig. 9: Root-mean-square of wavefront reconstructions as a function of WFC iteration from eight on-orbit wavefront control experiments run in June 2021. In each experiment, the DeMi payload successfully reduced the RMS wavefront error from $\sim$ 450 nm to less than 150 nm. Data is labeled according to the time that the file was saved on the payload in UTC.

example of using CubeSats to demonstrate new technology for space applications.

The data presented in this paper show that the DeMi payload MEMS DM and miniature DM driver are operating in space with similar performance compared to ground testing. Downlinked spotfield data from the SHWFS camera with the internal laser source shows that the DeMi optical system has not shifted significantly since launch.

Actuator deflection data show that the DM is operating in space with no unresponsive actuators detected among the actuators visible with the internal laser source. The deflection data shows that the DM response to command voltage in space has good agreement with ground data from environmental testing with the same level of measurement uncertainty. The measured deflection amount appears to have a dependence on payload temperature, with lower

temperature experiments resulting in up to 200 nm smaller deflection measurements at a commanded poke voltage of 150 V. The DeMi SHWFS with the internal laser source has been shown to meet the 12 nm precision requirement for individual actuator deflections for commanded poke voltages up to 120 V with both in-space data and environmental testing data. Measurements with the SHWFS in space have been shown to be very repeatable with the standard deviation of single actuator measurements from two experiments of the same type ranging from 3-16 nm.

Wavefront control experiments with the DeMi SHWFS show that the payload can successfully and repeatably reduce the RMS wavefront error from $\sim$ 450 nm to less than 150 nm over nine iterations of wavefront control. This is the first known demonstration of wavefront control in space with a MEMS DM. The payload requirement is to control wavefront error to less than 100 nm RMS, and the DeMi team plans to accomplish this by running wavefront control experiments with more iterations in the future.

The next goal for the DeMi mission is to point the payload at a star and demonstrate wavefront control with the SHWFS using external starlight instead of the internal laser source. The DeMi team also plans to use the image plane sensor to monitor the impact of wavefront control on the payload PSF measurements and to perform image-plane wavefront sensing [28].

Acknowledgments

This material is based upon work supported by the Defense Advanced Research Projects Agency (DARPA) Program Office under Contract No. W31P4Q-16-C-0089. The DeMi mission is managed by Aurora Flight Sciences. The DeMi bus was built by Blue Canyon Technologies.

DeMi spacecraft environmental testing was conducted at the MIT Lincoln Laboratory Environmental Testing Laboratory. ETL staff including Kelly Beattie, Ron Efromson, Scott Hillis, Jon Howell, and Joseph Orender provided invaluable expertise throughout spacecraft testing. Chris Chesbrough from MIT Lincoln Laboratory was instrumental in helping the DeMi team with bonding of optical components.

Nanoracks LLC was the launch provider for the DeMi spacecraft and provided equipment and instruction for spacecraft vibration testing.

The MIT Kavli Institute generously provided access to an interferometer and clean room space for DeMi alignment and spacecraft testing.

Rachel Morgan is a NASA Space Technology Research Fellow under grant 80NSSC18K1182. Yinzi Xin is a NSF Graduate Research Fellow under grant 1122374.

This research made use of POPPY, an open-source optical propagation Python package originally developed for the James Webb Space Telescope [37]. This research also made use of Numpy[38] and Astropy,[1] a community-developed core Python package for Astronomy [39].

[1] Rachel E. Morgan, Ewan S. Douglas, Gregory Allan, Paula do Vale Pereira, Jennifer N. Gubner, Christian Haughwout, Christian Haughwout, Thomas Murphy, John Merk, Mark D. Egan, Gábor Furész, Danilo Roascio, Yinzi Xin, and Kerri L. Cahoy. Optical calibration and first light for the deformable mirror demonstration mission CubeSat (DeMi). *Journal of Astronomical Telescopes, Instruments, and Systems*, 7(2):1 – 20, 2021.

[2] Brendan Crill, Nick Siegler, Shawn Domagal-Goldman, Eric Mamajek, and Karl Stapelfeldt. Key Technology Challenges for the Study of Exoplanets and the Search for Habitable Worlds. Technical report, 2018. URL: https://arxiv.org/pdf/1803.04457.pdf.

[3] D. Grosse, F. Bennet, and M. Copeland et al. Adaptive optics for satellite imaging and earth based space debris maneuvers. In *Proc. 7th European Conference on Space Debris*, 2017.

[4] Craig Underwood, Sergio Pellegrino, Vaios Lappas, and et al. Using CubeSat/micro-satellite technology to demonstrate the Autonomous Assembly of a Reconfigurable Space Telescope (AAReST). *Acta Astronautica*, 114:112 – 122, 2015.

[5] Thomas Bifano. Adaptive imaging mems deformable mirrors. *Nature Photonics*, 5(1):21–23, 2011.

[6] Wesley A Traub, Ben R Oppenheimer, and Sara (Ed.) Seager. Direct Imaging of Exoplanets. In *Exoplanets*, pages 111–156. 2010.

[1] http://www.astropy.org

[7] Gael Chauvin, Anne-Marie Lagrange, H. Beust, Mickael Bonnefoy, Anthony Boccaletti, Daniel Apai, France Allard, David Ehrenreich, Julien H. V. Girard, David Mouillet, and D. Rouan. Pictoris b giant planet. *Astronomy & Astrophysics*, 542:A41, 2012.

[8] B. R. Oppenheimer, C. Baranec, C. Beichman, D. Brenner, R. Burruss, E. Cady, J. R. Crepp, R. Dekany, R. Fergus, D. Hale, L. Hillenbrand, S. Hinkley, David W. Hogg, D. King, E. R. Ligon, T. Lockhart, R. Nilsson, I. R. Parry, L. Pueyo, E. Rice, J. E. Roberts, L. C. Roberts, M. Shao, A. Sivaramakrishnan, R. Soummer, T. Truong, G. Vasisht, A. Veicht, F. Vescelus, J. K. Wallace, C. Zhai, and N. Zimmerman. Reconnaissance of the hr 8799 exosolar system. I. near-infrared spectroscopy. *Astrophysical Journal*, 768(24), 2013.

[9] Sara Seager and Drake Deming. Exoplanet Atmospheres. *Annual Review of Astronomy and Astrophysics*, 48:631–672, 2010.

[10] Bijan Nemati, Mark T. Stahl, H. Philip Stahl, and Stuart B. Shaklan. Effects of space telescope primary mirror segment errors on coronagraph instrument performance. In *Proceedings of SPIE 10398 UV/Optical/IR SPace Telescopes and Instruments: Innovative Technologies and Concepts VIII*, 2017.

[11] Laurent Pueyo and N. Jeremy Kasdin. Polychromatic Compensation of Propagated Aberrations for High-Contrast Imaging. *The Astrophysical Journal*, 666(1):609–625, 2007.

[12] John T. Trauger and Wesley A. Traub. A laboratory demonstration of the capability to image an Earth-like extrasolar planet. *Nature*, 446(7137):771–773, 2007.

[13] F. Malbet, W. Yu, J., and M. Shao. High-Dynamic-Range Imaging Using a Deformable Mirror for Space Coronography. *Publications of the Astronomical Society of the Pacific*, 107:386–398, 1995.

[14] Katie M. Morzinski, Julia W. Evans, Scott Severson, Bruce Macintosh, Daren Dillon, Don Gavel, Claire Max, and Dave Palmer. Characterizing the potential of MEMS deformable mirrors for astronomical adaptive optics. In *Proceedings of SPIE 6272 Advances in Adaptive Optics II*, 2006.

[15] Michael A. Helmbrecht, Min He, Carl J. Kempf, and Marc Besse. MEMS DM development at Iris AO, Inc. In *Proceedings of SPIE 7931 MEMS Adaptive Optics V*, 2011.

[16] Rachel Morgan, Ewan Douglas, Gregory Allan, Paul Bierden, Subriya Chakrabarti, Timothy Cook, Mark Egan, Gabor Furesz, Jennifer Gubner, Tyler Groff, Christian Haughwout, Bobby Holden, Christopher Mendillo, Mireille Ouellet, Paula do Vale Pereira, Abigail Stein, Simon Thibault, Xingtao Wu, Yeyuan Xin, and Kerri Cahoy. MEMS Deformable Mirrors for Space-Based High Contast Imaging. *Micromachines*, 366(10), 2019.

[17] Ewan S. Douglas, Christopher B. Mendillo, Timothy A. Cook, Kerri L. Cahoy, and Supriya Chakrabarti. Wavefront sensing in space: flight demonstration II of the PICTURE sounding rocket payload. *Journal of Astronomical Telescopes, Instruments, and Systems*, 4(1):1 – 10, 2018.

[18] Timothy Cook, Kerri Cahoy, Supriya Chakrabarti, Ewan Douglas, Susanna C. Finn, Marc Kuchner, Nikole Lewis, Anne Marinan, Jason Martel, Dimitri Mawet, Benjamin Mazin, Mark Swain, Seth R. Meeker, Christopher Mendillo, David Stuchlik, and Gene Serabyn. Planetary Imaging Concept Testbed Using a Recoverable Experiment - Coronagraph (PICTURE C). *Journal of Astronomical Telescopes, Instruments, and Systems*, 1(4):044001, 2015.

[19] Olivier Côté, Guillaume Allain, Denis Brousseau, Marie-Pier Lord, Samy Ouahbi, Mireille Ouellet, Deven Patel, Simon Thibault, CÃ©dric Vallée, Ruslan Belikov, Eduardo A. Bendek, CÃ©lia Blain, Collin Bradley, Olivier Daigle, Chris de Jong, David Doelman, RenÃ© Doyon, FrÃ©dÃ©ric Grandmont, Michael Helmbrecht, Matthew A. Kenworthy, David Lafrenière, Frank Marchis, Christian Marois, Steeve Montminy, Frans Snik, Gautam Vasisht, Jean-Pierre Véran, and Philippe Vincent. A precursor mission to high contrast imaging balloon system. In *Proceedings of SPIE 10702 Ground-based and Airborne Instrumentation for Astronomy VII*, 2018.

[20] Gregory W Allan. Simulation and Testing of Wavefront Reconstruction Algorithms for the Deformable Mirror (DeMi) Cubesat. Master's thesis, 2018. URL: https://dspace.mit.edu/handle/1721.1/120381.

[21] Kerri L. Cahoy, Anne D. Marinan, Benjamin Novak, Caitlin Kerr, Tam Nguyen, Matthew Webber, Grant Falkenburg, and Andrew Barg. Wavefront control in space with MEMS deformable mirrors for exoplanet direct imaging. *Journal of Micro/Nanolithography, MEMS, and MOEMS*, 13(1), 2014.

[22] Anne Marinan and Kerri Cahoy. CubeSat Deformable Mirror Demonstration. In *International Symposium on Optomechatronic Technologies*, 2014.

[23] Anne Marinan, Kerri Cahoy, John Merck, Ruslan Belikov, and Eduardo Bendek. Improving Nanosatellite Imaging with Adaptive Optics. In *Proceedings of AIAA/USU Conference on Small Satellites*, 2016.

[24] Ewan S. Douglas, Gregory Allan, Derek Barnes, Joseph S. Figura, Christian A. Haughwout, Jennifer N. Gubner, Alex A. Knoedler, Sarah LeClair, Thomas J. Murphy, Nikolaos Skouloudis, John Merck, Roedolph A. Opperman, and Kerri L. Cahoy. Design of the deformable mirror demonstration CubeSat (DeMi). In *Proceedings of SPIE*

10400 Techniques and Instrumentation for Detection of Exoplanets, 2017.

[25] Ewan S. Douglas, Gregory Allan, Derek Barnes, Joseph S. Figura, Christian A. Haughwout, Jennifer N. Gubner, Alex A. Knoedler, Sarah LeClair, Thomas J. Murphy, Nikolaos Skouloudis, John Merck, Roedolph A. Opperman, and Kerri Cahoy. Design of the deformable mirror demonstration CubeSat (DeMi). In *Proceedings of SPIE 10400 Techniques and Instrumentation for Detection of Exoplanets*, 2017.

[26] Jennifer Gubner. Payload Configuration , Integration and Testing of the Deformable Mirror Demonstration Mission (DeMi) CubeSat. In *32nd Annual AIAA/USU Conference on Small Satellites*, 2018.

[27] Jennifer Gubner. Deformable Mirror Demonstration Mission. B. S. thesis, 2018. URL: https://repository.wellesley.edu/thesiscollection/606.

[28] Gregory Allan, Ewan S. Douglas, Derek Barnes, Mark Egan, Gabor Furesz, Warren Grunwald, Jennifer Gubner, Bobby G. Holden, Christian Haughwout, Paula do Vale Pereira, Abigail J. Stein, and Kerri L. Cahoy. The deformable mirror demonstration mission (DeMi) CubeSat: optomechanical design validation and laboratory calibration. 1069857(August 2018):180, 2018.

[29] Paula do Vale Pereira, B Holden, R Morgan, and et. al. Thermomechanical design and testing of the Deformable Mirror Demonstration Mission (DeMi) CubeSat. In *Proceedings of the 2020 AIAA/USU Conference on Small Satellites*, 2020.

[30] Jennifer Gubner. The Deformable Mirror Demonstration Mission (DeMi) On-Orbit Analysis. Master's thesis, 2021.

[31] Ewan S. Douglas, Greg Allan, Rachel Morgan, Bobby G. Holden, Jennifer Gubner, Christian Haughwout, Paula do Vale Pereira, Yinzi Xin, John Merk, and Kerri L. Cahoy. Small mirrors for small satellites: Design of the deformable mirror demonstration mission cubesat (demi) payload. *Frontiers in Astronomy and Space Sciences*, 8:126, 2021.

[32] Rachel Morgan. Payload Configuration , Integration and Testing of the Deformable Mirror Demonstration Mission (DeMi) CubeSat. In *34th Annual AIAA/USU Conference on Small Satellites*, 2020.

[33] Rachel Morgan. Optical modeling and validation for the Deformable Mirror Demonstration Mission. Master's thesis, 2020. URL: https://dspace.mit.edu/handle/1721.1/128059.

[34] Christian Haughwout. Electronics Development for the Deformable Mirror Demonstration Mission (DeMi). Master's thesis, 2018. URL: https://dspace.mit.edu/handle/1721.1/120438.

[35] W.H. Southwell. Wave-front estimation from wave-front slope measurements. *J. Opt. Soc. Am.*, 70(8):998–1006, Aug 1980.

[36] Guang-ming Dai. *Wavefront Optics for Vision Correction*. SPIE, 2008.

[37] Marshall D. Perrin, Remi Soummer, Erin M. Elliott, Matthew D. Lallo, and Anand Sivaramakrishnan. Simulating point spread functions for the James Webb Space Telescope with WebbPSF. In Mark C. Clampin, Giovanni G. Fazio, Howard A. MacEwen, and Jacobus M. Oschmann Jr., editors, *Space Telescopes and Instrumentation 2012: Optical, Infrared, and Millimeter Wave*, volume 8442, pages 1193 – 1203. International Society for Optics and Photonics, SPIE, 2012.

[38] Charles R. Harris, K. Jarrod Millman, St'efan J. van der Walt, Ralf Gommers, Pauli Virtanen, David Cournapeau, Eric Wieser, Julian Taylor, Sebastian Berg, Nathaniel J. Smith, Robert Kern, Matti Picus, Stephan Hoyer, Marten H. van Kerkwijk, Matthew Brett, Allan Haldane, Jaime Fern'andez del R'ıo, Mark Wiebe, Pearu Peterson, Pierre G'erard-Marchant, Kevin Sheppard, Tyler Reddy, Warren Weckesser, Hameer Abbasi, Christoph Gohlke, and Travis E. Oliphant. Array programming with NumPy. *Nature*, 585(7825):357–362, September 2020.

[39] The Astropy Collaboration, A. M. Price-Whelan, and B. M. Siphocz et al. The Astropy Project: Building an Open-science Project and Status of the v2.0 Core Package.
aj, 156:123, September 2018.